



This is a repository copy of *Critical plane and critical distance approaches to assess damage under variable amplitude fretting fatigue loading*.

White Rose Research Online URL for this paper:

<https://eprints.whiterose.ac.uk/184774/>

Version: Accepted Version

---

**Proceedings Paper:**

Teuchou Kouanga, C.V., Nowell, D., Dwyer Joyce, R.S. et al. (1 more author) (2022) Critical plane and critical distance approaches to assess damage under variable amplitude fretting fatigue loading. In: Wahab, M.A., (ed.) Proceedings of the 9th International Conference on Fracture, Fatigue and Wear - FFW 2021. 9th International Conference on Fracture, Fatigue and Wear, 02-03 Aug 2021, Ghent University, Belgium. Lecture Notes in Mechanical Engineering . Springer, Singapore , pp. 161-173. ISBN 9789811688096

[https://doi.org/10.1007/978-981-16-8810-2\\_13](https://doi.org/10.1007/978-981-16-8810-2_13)

---

This is a post-peer-review, pre-copyedit version of an article published in Proceedings of the 9th International Conference on Fracture, Fatigue and Wear. The final authenticated version is available online at: [http://dx.doi.org/10.1007/978-981-16-8810-2\\_13](http://dx.doi.org/10.1007/978-981-16-8810-2_13).

**Reuse**

Items deposited in White Rose Research Online are protected by copyright, with all rights reserved unless indicated otherwise. They may be downloaded and/or printed for private study, or other acts as permitted by national copyright laws. The publisher or other rights holders may allow further reproduction and re-use of the full text version. This is indicated by the licence information on the White Rose Research Online record for the item.

**Takedown**

If you consider content in White Rose Research Online to be in breach of UK law, please notify us by emailing [eprints@whiterose.ac.uk](mailto:eprints@whiterose.ac.uk) including the URL of the record and the reason for the withdrawal request.



[eprints@whiterose.ac.uk](mailto:eprints@whiterose.ac.uk)  
<https://eprints.whiterose.ac.uk/>

# Critical plane and critical distance approaches to assess damage under variable amplitude fretting fatigue loading

C.V. Teuchou Kouanga<sup>1</sup>, D. Nowell<sup>2</sup>, R. S. Dwyer–Joyce<sup>3</sup> and L. Susmel<sup>1</sup>

<sup>1</sup>Department of Civil and Structural Engineering,  
the University of Sheffield, Sheffield, S1 3JD, UK

<sup>2</sup>Department of Mechanical Engineering, Imperial College London,  
London, SW7 2AZ, UK

<sup>3</sup>Department of Mechanical Engineering, the University of Sheffield, Sheffield, S1 3JD, UK  
l.susmel@sheffield.ac.uk

**Abstract.** This paper summarises an attempt to formulate a design approach suitable for predicting the finite lifetime of mechanical assemblies subjected to constant/variable amplitude fretting fatigue loading. The proposed design methodology makes use of the Modified Wöhler Curve Method (MWCM), applied in conjunction with the Theory of Critical Distance (TCD) and the Shear Stress-Maximum Variance Method ( $\tau$ -MVM). In particular, the TCD (applied in the form of the Point Method) is used to take into account the damaging effect of the multi-axial stress gradients acting on the material in the vicinity of the contact region. The time-variable linear-elastic stress state at the critical point is then post-processed according to the MWCM which is a bi-parametrical criterion that estimates fatigue lifetime via the planes experiencing the maximum shear stress amplitude. Finally, the  $\tau$ -MVM is used to calculate the stress quantities relative to the critical plane whose orientation is determined numerically by selecting the plane containing the direction experiencing the maximum variance of the resolved shear stress. Further, this direction is also used to perform the cycle counting by directly applying the classic Rain-Flow Method to post-process the resolved shear stress. The overall accuracy and reliability of the proposed approach is checked against a large number of new experimental results that were generated in the Sheffield Structures Laboratory under variable amplitude fretting fatigue loading.

**Keywords:** Fretting fatigue prediction, Theory of Critical Distance, multiaxial fatigue.

## 1 Introduction

Fretting fatigue damage is a term used to describe those failures occurring in mechanical components at the contact interfaces, with this damage mechanism being active in the presence of combined reciprocating frictional contacts and remote fatigue loading. Over the years, fretting fatigue cracks have been observed in numerous real mechanical

assemblies such as, for instance, cylinder block/head gasket of internal combustion engines, threaded pipe connections, riveted/bolted joints and blade-disk attachments in turbine of aero engine [1]. Hence, the prediction of fretting fatigue lifetime of materials and components is of great interest in situations of industrial interest. This explains the reason why, numerous theoretical and experimental systematic studies have been carried out since the early 1960s to quantify and model damage in materials subjected to fretting fatigue loading. Examination of the state of art demonstrates that most fretting fatigue investigations have been conducted under constant amplitude (CA) load histories [2-9]. In particular, the majority of the experimental studies available in the technical literature consist of applying a static load to the testing pads and a CA fatigue load to the specimens. In contrast, very little experimental work has been done to investigate fretting fatigue failures under variable amplitude (VA) loading.

In the scenario briefly described above, the novelty characterising this investigation is twofold. Firstly, to generate new experimental results, where specimens made of cast iron are tested under VA and CA fretting fatigue loading. Secondly, by making use of the ‘‘notch analogue’’ concept [10], the MWCM in conjunction with the TCD and the Shear Stress-Maximum Variance Method ( $\tau$ -MVM) is used to estimate the finite lifetime of the laboratory specimens tested under both CA and VA fretting fatigue loading.

## 2 Fundamental of the MWCM under CA loading

The MWCM [11-12] is a critical plane approach which postulates that fatigue damage in materials subjected to fatigue loading can be quantified via the maximum shear amplitude,  $\tau_a$ , the mean normal stress,  $\sigma_{n,m}$ , and the normal stress amplitude,  $\sigma_{n,a}$ , relative to the material plane experiencing the maximum shear stress amplitude (i.e. the so-called critical plane). The stress components associated with the critical plane are used to assess the fatigue damage extent via the following ratio [13]:

$$\rho_{\text{eff}} = \frac{m \cdot \sigma_{n,m}}{\tau_a} + \frac{\sigma_{n,a}}{\tau_a} \quad (1)$$

According to the way this critical plane stress ratio is defined,  $\rho_{\text{eff}}$  is equal to unity under fully-reversed uniaxial fatigue loading and to zero under fully-reversed torsional fatigue loading [14-15]. In Eq. (1),  $m$  is the mean stress sensitivity index that ranges between 0 and 1. A material is said to be insensitive to the presence of superimposed static stresses when  $m=0$ , whereas  $m=1$  corresponds to a situation where the material is fully-sensitive to the presence of non-zero mean stresses [13].  $m$  is a material property that must be determined by running appropriate experiments.

The MWCM estimates fatigue damage via non-conventional SN curves that are plotted as  $\tau_a$  vs.  $N_f$  modified Wöhler diagrams. According to the log-log chart reported in Fig. 1, any modified Wöhler curve is defined via its reference shear stress amplitude,  $\tau_{A,\text{Ref}}(\rho_{\text{eff}})$ , extrapolated at  $N_{\text{Ref}}$  cycles to failure and its negative inverse slope,  $k_{\tau}(\rho_{\text{eff}})$ . According to the scheme shown in Fig. 1, fatigue damage is seen to increase as  $\rho_{\text{eff}}$  increases, since the corresponding fatigue curve tends to shift downwards with increasing  $\rho_{\text{eff}}$  (Fig. 1a). According to the classical log-log scheme used to summarise fatigue data, the position and the negative inverse slope of any Modified Wöhler curve can be defined through the following linear relationships [14]:

$$K_{\tau}(\rho_{\text{eff}}) = (k - k_0)\rho_{\text{eff}} + k_0 \text{ for } \rho_{\text{eff}} \leq \rho_{\text{lim}} \quad (2)$$

$$\tau_{A,\text{Ref}}(\rho_{\text{eff}}) = \left(\frac{\sigma_A}{2} - \tau_A\right)\rho_{\text{eff}} + \tau_A \text{ for } \rho_{\text{eff}} \leq \rho_{\text{lim}} \quad (3)$$

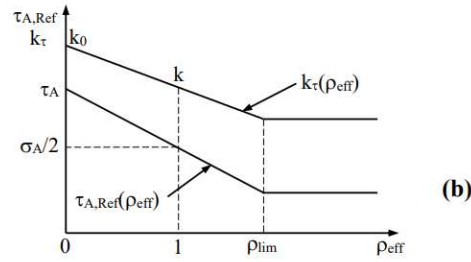
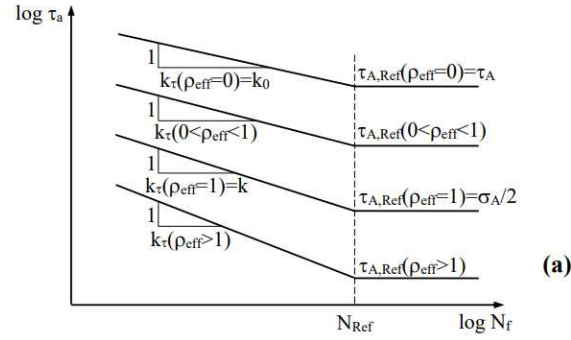


**Fig. 1.** Modified Wöhler diagram (a) and variation of  $k_{\tau}$  and  $\tau_{A,\text{Ref}}$  with  $\rho_{\text{eff}}$ .

The meaning of the symbols used in the above relationships is explained in Fig. 1. For the sake of clarity, Eqs (2) and (3) are also plotted in Fig. 1b. This schematic diagram can be used to introduce another important assumption that is made to deal effectively with those situations involving large values of ratio  $\rho_{\text{eff}}$ . In particular, the schematic chart of Fig. 1b makes it evident that when  $\rho_{\text{eff}}$  is larger than  $\rho_{\text{lim}}$ ,  $k_{\tau}(\rho_{\text{eff}})$  and  $\tau_{A,\text{Ref}}(\rho_{\text{eff}})$  take on the following values [13, 15]:

$$K_{\tau}(\rho_{\text{eff}}) = (k - k_0)\rho_{\text{lim}} + k_0 = \text{const} \text{ for } \rho_{\text{eff}} > \rho_{\text{lim}} \quad (4)$$

$$\tau_{A,\text{Ref}}(\rho_{\text{eff}}) = \left(\frac{\sigma_A}{2} - \tau_A\right)\rho_{\text{lim}} + \tau_A = \text{const} \text{ for } \rho_{\text{eff}} > \rho_{\text{lim}} \quad (5)$$

where [13]:

$$\rho_{\text{lim}} = \frac{\tau_A}{2\tau_A - \sigma_A} \quad (6)$$

The above correction, which plays a key role in the overall accuracy of the MWCM, was introduced as a consequence of the fact that, under large values of ratio  $\rho_{\text{eff}}$ , the

estimates obtained via the conventional critical plane approach are seen to become too conservative [15]. According to the experimental results due to Kaufman and Topper [16], such a high degree of conservatism can be ascribed to the fact that, when micro/meso cracks are fully open, an increase of the normal mean stress does not result in a further increase of fatigue damage. This important damage mechanism is incorporated into the MWCM via the use of  $\rho_{lim}$  together with relationships (4) and (5) [13].

As far as CA multiaxial fatigue assessment is concerned, the modified Wöhler diagram of Fig. 1a can directly be used to estimate fatigue life via the following trivial relationship:

$$N_f = \left[ \frac{\tau_{A,Ref}(\rho_{eff})}{\tau_a} \right]^{K_\tau(\rho_{eff})} \quad (7)$$

In Eq. (7),  $\tau_a$  and  $\rho_{eff}$  are to be determined by post-processing the stress components relative to the critical plane, whereas  $\tau_{A,Ref}(\rho_{eff})$  and  $k_\tau(\rho_{eff})$  are directly estimated from Eqs (2) to (5).

### 3 The MWCM applied along the TCD to estimate VA fretting fatigue lifetime

In order to increase its computational efficiency, the MWCM is recommended for application by defining the critical plane as that material plane containing the direction experiencing the maximum variance of the resolved shear stress [17-19]. Accordingly, in this paper, the Shear Stress-Maximum Variance Method ( $\tau$ -MVM) [20] will be used to calculate the orientation of the critical plane and the associated stress components. Since the algorithm to determine the critical plane according to  $\tau$ -MVM has already been discussed in detail elsewhere [19, 20], only the definitions used to calculate  $\tau_a$ ,  $\sigma_{n,m}$  and  $\sigma_{n,a}$  will be recalled briefly below. Further, in what follows, the use of the MWCM applied along with the Theory of Critical Distances (TCD) [21, 22] will be reformulated for the fretting fatigue VA case, with the CA fretting fatigue problem [22] being just a simpler sub-case of the more complex VA solution [23].

The procedure for the in-field usage of the MWCM/TCD is summarised in Figs 2 and 3. In particular, for the sake of simplicity, consider the flat specimen sketched in Fig. 2. This specimen is loaded by an axial cyclic stress,  $\Delta\sigma_b$ , and two fretting pads are pushed against the specimen itself by force,  $P$ . The two pads are subjected also to an oscillatory tangential force,  $\Delta Q$ .

According to the TCD [6, 22-24], the focus path is defined as a straight line that emanates from the trailing edge of the contact zone (point A in Fig. 2) and is perpendicular to the contact surface itself. If the TCD is applied in the form of the Point Method (PM) [25], the linear-elastic stress state to be used to estimate fatigue damage is taken at a distance from the assumed crack initiation point (i.e., point A in Fig. 2) equal to  $L_M(N_f)/2$  where [21, 22]:

$$L_M(N_f) = A \cdot N_f^B \quad (8)$$

In Eq. (8), A and B are material fatigue constants to be determined by running appropriate experiments. The experimental strategies suitable for estimating A and B are discussed in detail in Refs [21, 22].

Since, according to relationship (8), the critical distance,  $L_M$ , is a function of the number of cycles to failure,  $N_f$ , the design approach proposed in the present section is applied by adopting suitable recursive procedures so that convergence can be reached effectively and unambiguously [21, 22].

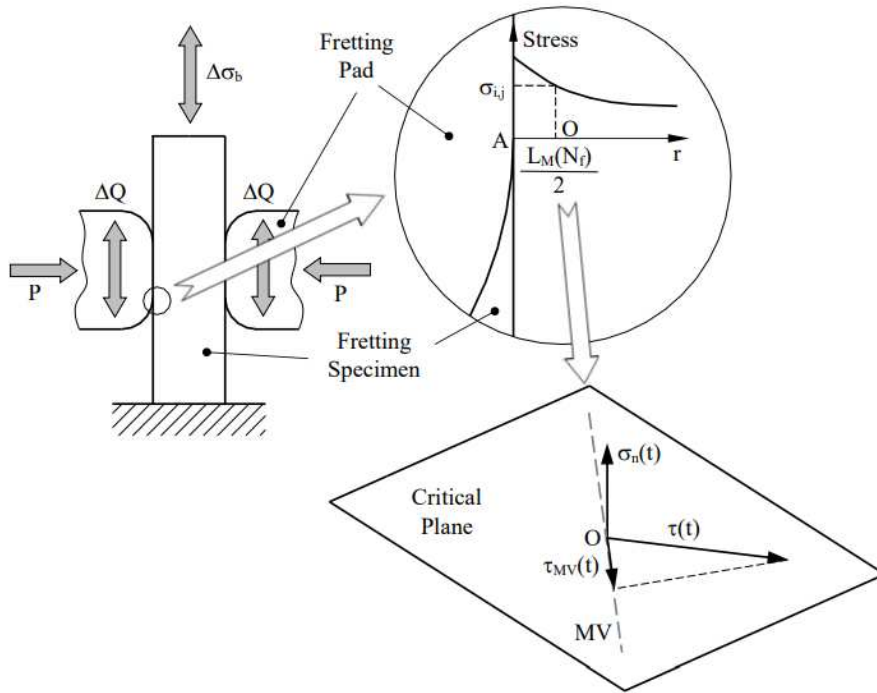


**Fig. 2.** The MWCM applied in conjunction with the PM and the  $\tau$ -MVM to estimate, along the focus path, the stress components relative to the critical plane.

Assume now that the point  $O$  along the focus path is the point of interest and its distance from the assumed crack initiation location is equal to  $L_M(N_f)/2$ . From the linear-elastic stress state at point  $O$ , the orientation of the critical plane is determined by locating that material plane containing the direction experiencing the maximum variance of the resolved shear stress (direction  $MV$  in Fig. 2) [20, 23]. The shear stress amplitude relative to the critical plane,  $\tau_a$ , can then be calculated from the variance of the shear stress resolved along direction  $MV$ ,  $\tau_{MV}(t)$ , i.e. [20]:

$$\begin{aligned} \tau_m &= \frac{1}{T} \int_0^T \tau_{MV}(t) \cdot dt; \text{Var}[\tau_{MV}(t)] = \frac{1}{T} \int_0^T [\tau_{MV}(t) - \tau_m]^2 \cdot dt \Rightarrow \\ &\Rightarrow \tau_a = \sqrt{2 \cdot \text{Var}[\tau_{MV}(t)]} \end{aligned} \quad (9)$$

where  $T$  is the time interval over which the assessed load history is defined (Fig. 3a). In a similar way, the mean value,  $\sigma_{n,m}$ , and the amplitude,  $\sigma_{n,a}$ , of the stress,  $\sigma_n(t)$ , normal to the critical plane (Figs 2 and 3b) take on the following values [20]:

$$\begin{aligned} \sigma_{n,m} &= \frac{1}{T} \int_0^T \sigma_n(t) \cdot dt; \text{Var}[\sigma_n(t)] = \frac{1}{T} \int_0^T [\sigma_n(t) - \sigma_{n,m}]^2 \cdot dt \Rightarrow \\ &\Rightarrow \sigma_{n,a} = \sqrt{2 \cdot \text{Var}[\sigma_n(t)]} \end{aligned} \quad (10)$$

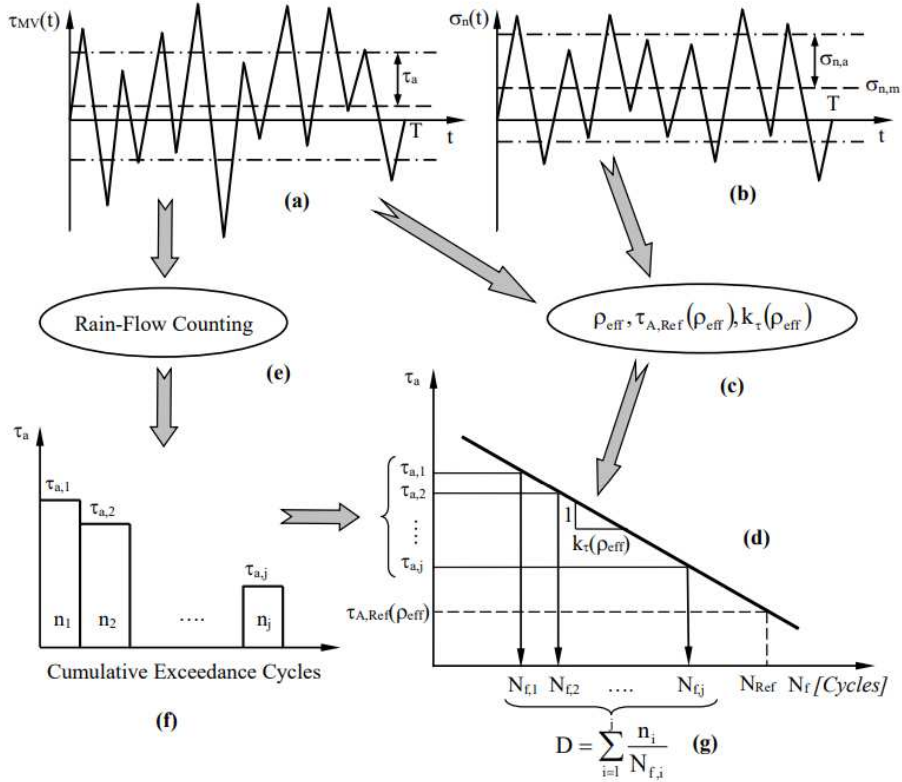


**Fig. 3.** Procedure to estimate damage under VA fatigue loading according to the MWCM.

As soon as  $\tau_a$ ,  $\sigma_{n,m}$  and  $\sigma_{n,a}$  are known, the degree of multiaxiality and non-proportionality of the stress state at point O can directly be evaluated in terms of ratio  $\rho_{\text{eff}}$  (Fig. 3c), with the position of the corresponding modified Wöhler curve being estimated according to relationships (2) to (5) - (Fig. 3d). By making use of the classical rainflow method [26], the resolved shear stress cycles can now be counted (Figs 3a and 3e) to build the corresponding load spectrum (Fig. 3f). Finally, the calculated load spectrum has to be used to estimate the damage content associated with any counted shear stress level (Figs. 3f, 3d and 3g), i.e.:

$$D = \sum_{i=1}^j \frac{n_i}{N_{f,i}} \quad (11)$$

Subsequently, total damage  $D$  is used to determine an equivalent number of cycles to failure,  $N_{f,eq}$ , to be used to estimate the critical distance value via Eq. (8), where [23]:

$$N_{f,eq} = \frac{\sum_{i=1}^j n_i}{\sum_{i=1}^j \frac{n_i}{N_{f,i}}} \quad (12)$$

Accordingly, the  $L_M$  vs.  $N_f$  relationship defined according to Eq. (8) can be rewritten directly as [23]:

$$L_M(N_{f,eq}) = A \cdot N_{f,eq}^B = A \cdot \left( \frac{\sum_{i=1}^j n_i}{\sum_{i=1}^j \frac{n_i}{N_{f,i}}} \right)^B \quad (13)$$

where constants  $A$  and  $B$  are those estimated for the material being assessed by following the standard procedures being discussed in Refs [21, 22].

If the  $L_M$  value estimated via Eq. (13) assures the following obvious condition:

$$\frac{L_M(N_{f,eq})}{2} - r = 0 \quad (14)$$

where, according to Fig. 2,  $r$  is the distance, measured along the focus path, from crack initiation point  $A$ , then the number of cycles to failure,  $N_{f,e}$ , can be estimated directly as [23]:

$$N_{f,e} = \frac{D_{cr}(\rho_{eff}) \cdot n_{tot}}{D} = \frac{D_{cr}(\rho_{eff}) \cdot \sum_{i=1}^j n_i}{\sum_{i=1}^j \frac{n_i}{N_{f,i}}} \quad (15)$$

In Eq. (15),  $D_{cr}(\rho_{eff})$  is the critical value of the damage sum. In contrast, if condition (13) is not assured, the same procedure as the one described above has to be re-applied by post-processing the stress state at a different point,  $O$ , along the focus path. This recursive procedure has to be re-used iteratively until convergence has occurred.

To conclude, it can be pointed out that in relationship (15)  $D_{cr}(\rho_{eff})$  is the critical value of damage sum  $D$  and the hypothesis is formed that, in the most general case,  $D_{cr}(\rho_{eff})$  can vary as the degree of multiaxiality and non-proportionality of the assessed stress state changes [23]. In contrast, if fatigue lifetime is estimated according to the classical rule due to Palmgren [26] and Miner [27], then the critical value of the damage sum can be taken invariably equal to unity.

## 4 Experimental investigation

### 4.1 Calibration of the MWCM's governing equations and the $L_M$ vs. $N_f$ relationship

In order to validate the fretting fatigue design method summarised in Figs 2 and 3, a number of experimental results were generated by testing specimens made of a cast iron commonly used in the automotive industry.

To calibrate the MWCM governing equations for the cast iron under investigation, a comprehensive experimental material characterisation was carried out using a 100kN Mayes fatigue testing machine as well as a SCHENCK servo-controlled closed-loop axial-torsion fatigue machine with maximum axial load capacity of 400 kN and maximum torque capacity of 1000 Nm. The force/torque-controlled tests were run using sinusoidal loading signals, with the frequency varying in the range 5-10 Hz. Fatigue failures were defined by 20% stiffness drop.

The results generated under the fully-reversed uniaxial fatigue loading were used to estimate  $\sigma_A$  and  $k$ , with fatigue constants  $\tau_A$  and  $k_0$  being determined from the tests run under fully-reversed torsional fatigue loading. The mean stress sensitivity index,  $m$ , for the cast iron under investigation was estimated according to the procedure described in Refs [22, 25], with this being done by taking full advantage of a further plain fatigue curve experimentally determined under  $R=0.1$ .

The strategy summarised in Refs [21, 25] was used to calculate material constants  $A$  and  $B$  in the  $L_M$  vs.  $N_f$  relationship, Eq. (8). In more detail, constants  $A$  and  $B$  were directly estimated from the plain material fully-reversed uniaxial fatigue curve and a fatigue curve generated by testing under tension/compression ( $R=-1$ ) specimens containing a known geometrical feature.

## 4.2 Fretting fatigue experiments

Fretting fatigue experimental tests were carried out using the hydraulic rig located at the Materials Testing Laboratory of the University of Sheffield that is shown in Fig. 4. The testing rig being used comprises of a Moog controller, two horizontal actuators and two vertical actuators. The horizontal actuators were used to apply the CA/VA axial cyclic force,  $F$ , to the flat-dog-bone specimens made of the cast iron under investigation.

Two different sets of pads were used. The first set was machined from steel and the second from cast iron. All pads were cylindrical with thickness equal to 12 mm, contact radius,  $R_p$ , equal to 75 mm and height equal to 15 mm. The experimental trials were run to investigate the different scenarios described in what follows.

In the first testing configuration, the two cylindrical pads were pushed against the fretting specimen by a static normal load,  $P$ . A fully-reversed CA sinusoidal load was then applied (at a frequency of 10 Hz) to one end of the specimen, while the other end was kept fixed.

In the second testing configuration, the two cylindrical pads were instead pushed against the fretting specimen by a CA sinusoidal normal load, with a fully-reversed CA sinusoidal axial load being applied to one end of the specimens. Both the normal and axial fatigue forces were in phase and applied at frequency of 10 Hz.

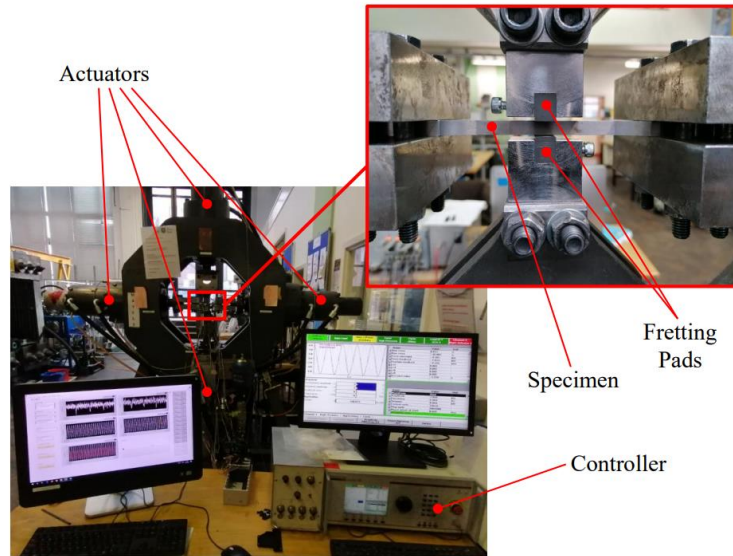


Fig. 4. Fretting fatigue test rig, specimens and pads.

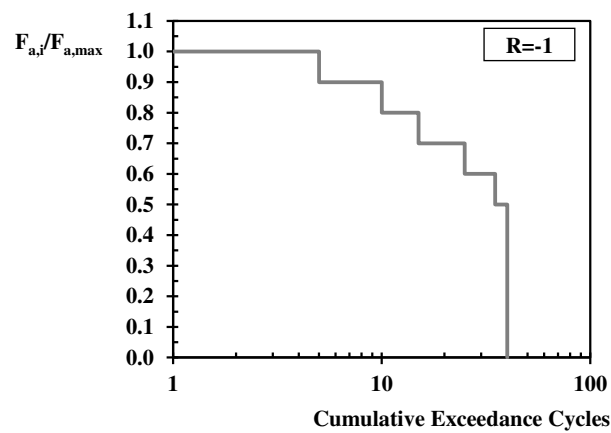


Fig. 5. Load spectrum adopted to run the VA fretting fatigue tests ( $F_{a,max}$ =maximum value of the amplitude of the force in the load spectrum;  $F_{a,i}$ =amplitude of the force associated with the  $i$ -th cycle).

In the final configuration, the dog-bone specimens were subjected to VA sinusoidal axial load histories, with the pads being used to apply a constant normal force. The VA load spectrum used to run the VA tests is shown in Fig. 5. The VA cycles were applied in random order at a frequency of 10 Hz and all load blocks contained 40 cycles.

## 5 Validation

The results generated from the fretting fatigue experiments summarised in the previous section were used to check the accuracy of the design methodology sketched in Figs 2 and 3. In order to predict the number of cycles to failure for each test, ANSYS Workbench® was used to estimate the linear elastic stress fields at the contact interface between pads and specimens. The stress fields obtained at the assumed crack initiation location were then post-processed according to the procedure proposed in Section 3. In the present investigation, the crack initiation point was taken at the trailing edge of the contact region.

As recommended by Palmgren [26] and Miner [27], the VA design method summarised in Figs 2 and 3 was applied by setting the critical value of the damage equal to unity.

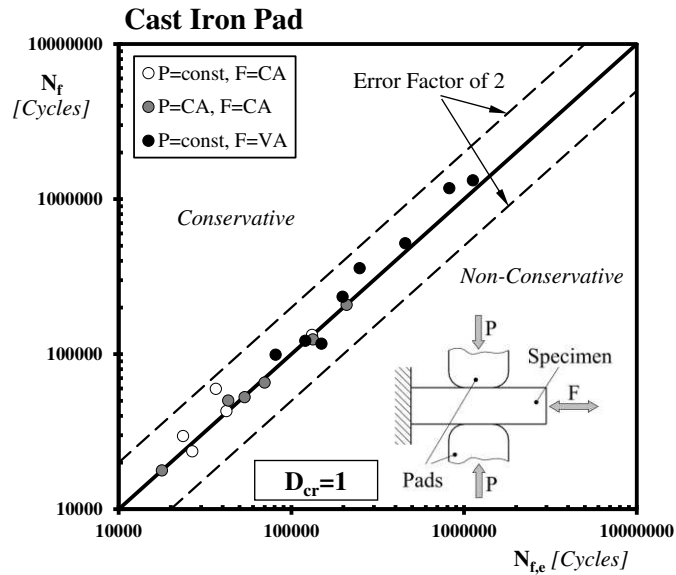


**Fig. 6.** Accuracy of the MWCM applied along with TCD and  $\tau$ -MVM in estimating the fretting fatigue results generated by using pads made of cast iron.

The experimental,  $N_f$ , vs. estimated,  $N_{fe}$ , number of cycles to failure diagrams reported in Figs 6 and 7 summarise the overall accuracy obtained by using the proposed fretting fatigue design methodology to post-process the experimental results being generated. The error diagrams of Figs 6 and 7 confirm that the MWCM applied along with the PM and  $\tau$ -MVM to predict fretting fatigue lifetime resulted in estimates falling within an error factor (in lifetime) of 2. This result is certainly satisfactory, especially in light of the fact that the proposed approach can be applied by directly post-processing the stress analysis results from conventional linear-elastic FE models.

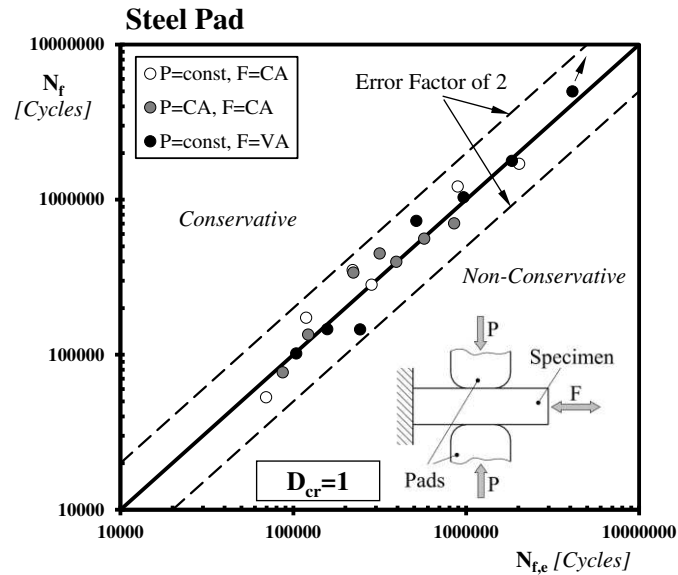


**Fig. 7.** Accuracy of the MWCM applied along with TCD and  $\tau$ -MVM in estimating the fretting fatigue results generated by using pads made of structural steel.

## 6 Conclusion

- The MWCM applied in conjunction with the  $\tau$ -MVM and the PM is seen to be highly accurate in predicting finite lifetime of cast iron subjected to both CA and VA fretting fatigue loading.
- The proposed approach is seen to be capable of modelling accurately the detrimental effect of different types of fretting fatigue loading configurations.
- Owing to the fact that the necessary stress analyses can be performed by solving standard linear-elastic FE models, the proposed fretting fatigue design technique is suitable for being used in situations practical interest.

## Acknowledgment

Support for this work from EPSRC ([www.epsrc.ac.uk](http://www.epsrc.ac.uk)) and Cummins Inc. ([www.cummins.com](http://www.cummins.com)) through the award of an Industrial CASE project is gratefully acknowledged.

## References

1. Jeung, H.K., Kwon, J.D., Lee, C.Y.: Crack initiation and propagation under fretting fatigue of inconel 600 alloy. *Journal Mechanical Science Technology* 29(12), 5241-5244 (2015).

2. Dini, D., Nowell, D., Dyson, I.N.: The use of notch and short crack approaches to fretting fatigue threshold prediction: Theory and experimental validation. *Tribology International* 39(8), 1158-1165 (2006).
3. Dini, D., Nowell, D., Dyson, I.N.: Experimental validation of a short crack approach for fretting fatigue threshold prediction. In: Pappalettere, C. (eds.) *Proceedings of the 12<sup>th</sup> International Conference on Experimental Mechanics*, Bari, Italy (2004).
4. Noraphaiphipaksa, L., Manonukul, A., Kanchanomai, C.: Fretting Fatigue with Cylindrical-On-Flat Contact: Crack Nucleation, Crack Path and Fatigue Life. *Materials (Basel)*. 2017 10(2) 155, 1-21 (2017) doi: 10.3390/ma10020155
5. Araújo, J.A., Susmel, L., Pires, M., Castro, F.: A multiaxial stress-based critical distance methodology to estimate fretting fatigue life. *Tribology International* 108, 2-6 (2017).
6. Araújo, J.A., Susmel, L., Taylor, D., Ferro, J., Mamiya, E.: On the use of the theory of critical distances and the Modified Wöhler curve method to estimate fretting fatigue strength of cylindrical contacts. *International Journal of Fatigue* 29, 95-107 (2007).
7. Araújo, J.A., Susmel, L., Taylor, D., Ferro, J.C.T., Ferreira, J.L.A.: On the prediction of High-Cycle Fretting Strength. Theory of Critical Distances vs. Hot spot Approach. *Engineering Fracture Mechanics* 75, 1763-1778 (2008).
8. Nowell, D.: An analysis of fretting fatigue (D.Phil.thesis). University of oxford, Oxford, UK (1988).
9. Hills, D., Nowell, D.: *Mechanics of Fretting Fatigue*. Kluwer Academic, Dordrecht, The Netherlands (1994).
10. Giannakopoulos, A.E., Lindley, T.C., Suresh, S.: Similarities of stress concentrations in contact at round punches and fatigue at notches: implications to fretting fatigue crack initiation. *Fatigue & Fracture of Engineering Materials & Structures* 23, 561-571 (2000).
11. Susmel, L., Tovo, R., Benasciutti D.: A novel engineering method based on the critical plane concept to estimate lifetime of weldments subjected to variable amplitude multiaxial fatigue loading. *Fatigue & Fracture of Engineering Materials & Structures* 32, 441-459 (2009).
12. Susmel, L., Lazzarin, P.: A Bi-parametric modified wöhler curve for high cycle multiaxial fatigue assessment. *Fatigue & Fracture of Engineering Materials & Structures* 25, 63-78 (2002).
13. Susmel, L.: Multiaxial fatigue limits and material sensitivity to non-zero mean stresses normal to critical planes. *Fatigue & Fracture of Engineering Materials & Structures* 31(3-4), 295-309 (2008).
14. Lazzarin, P., Susmel, L.: A stress-based method method to predict lifetime under multiaxial fatigue loadings. *Fatigue & Fracture of Engineering Materials & Structures* 26, 1171-1187 (2003).
15. Susmel, L., Tovo, R., Lazzarin, P.: The mean stress effect on the high-cycle fatigue strength from a multiaxial point of view. *International Journal of Fatigue* 27, 928-43 (2005).
16. Kaufman, R.P., Topper, T. The influence of static mean stresses applied normal to the maximum shear planes in multiaxial fatigue. In: Carpinteri, A., de Freitas, M., Spagnoli, A. (eds.) *Biaxial and multiaxial fatigue and fracture*, pp. 123-143. Elsevier and ESIS, Oxford, UK (2003).
17. Macha, E.: Simulation investigations of the position of fatigue fracture plane in materials with biaxial loads. *Materialwissenschaft und Werkstofftechnik* 20(4), 132-6 (1989).
18. Susmel, L., Tovo, R., Benasciutti, D.: A novel engineering method based on the critical plane concept to estimate lifetime of weldments subjected to variable amplitude multiaxial fatigue loading. *Fatigue & Fracture of Engineering Materials & Structures* 32, 441-59 (2009).

19. Susmel, L., Tovo, R.: Estimating fatigue damage under variable amplitude multiaxial fatigue loading. *Fatigue & Fracture of Engineering Materials & Structures* 34, 1053–77 (2011).
20. Susmel, L.: A simple and efficient numerical algorithm to determine the orientation of the critical plane in multiaxial fatigue problems. *International Journal of Fatigue* 32, 1875–83 (2010).
21. Susmel, L., Taylor, D., A novel formulation of the Theory of Critical Distances to estimate Lifetime of Notched Components in the Medium-Cycle Fatigue Regime. *Fatigue & Fracture of Engineering Materials & Structures* 30(7), 567-581 (2007).
22. Susmel, L., Taylor, D., The Modified Wöhler Curve Method applied along with the Theory of Critical Distances to estimate finite life of notched components subjected to complex multiaxial loading paths. . *Fatigue & Fracture of Engineering Materials & Structures* 31(12), 1047-1064, 2008.
23. Susmel, L., Taylor, D.: A critical distance/plane method to estimate finite life of notched components under variable amplitude uniaxial/multiaxial fatigue loading. *International Journal of Fatigue* 38, 7-24 (2012).
24. Kouanga, C. T., Jones, J. D., Reville, I., Wormald, A., Nowell, D., Dwyer-Joyce, R. S., Araújo, J. A., Susmel, L. On the estimation of finite lifetime under fretting fatigue loading. *International Journal of Fatigue* 112, 138-152, 2018.
25. Susmel, L.: *Multiaxial Notch Fatigue: from nominal to local stress-strain quantities*. Woodhead & CRC, Cambridge, UK (2009).
26. Matsuishi, M., Endo, T.: *Fatigue of metals subjected to varying stress*. Presented to the Japan Society of Mechanical Engineers. Fukuoka, Japan (1968).
27. Palmgren, A. Die Lebensdauer von Kugellagern. *Verfahrenstechnik*, Berlin, Germany, 68, 339-341 (1924).
28. Miner, M.A. Cumulative damage in fatigue. *Journal of Applied Mechanics* 67, AI59-AI64 (1945).